İSTANBUL UNIVERSITY
C E R R A H P A Ş A

Original Article

Post infectional alterations caused by *Xylaria polymorpha* in the secondary xylem of *Lannea coromandelica* (Houtt.) Merr

Lannea coromandelica (Houtt.) Merr'in sekonder ksileminde *Xylaria polymorpha* mantarının neden olduğu değişiklikler

Sivan Pramod[1] , Ajit M.Vasava[2] , Rina D. Koyani[3] , Kishore S. Rajput[2]

[1]Department of Forest Genetics and Plant Physiology, Umea Plant Science Centre, Swedish University of Agricultural Sciences, Umea, Sweden
[2]Department of Botany, Faculty of Science, The Maharaja Sayajirao University of Baroda, Vadodara, India
[3]School of Pharmacy, University of Texas at El Paso, Texas, USA

ABSTRACT

Xylaria polymorpha is known to cause root rot disease in hardwood trees. In the present study, trees of the species *Lannea coromandelica* infected with *X. polymorpha* showed symptoms consistent with root rot disease and also presented with a soft rot decay pattern. Bright-field microscopy, Confocal Microscopy, and Scanning Electron Microscopy revealed that fungal mycelia penetrated the S_2 layer of the fiber wall while axial parenchyma was found to be relatively resistant without much visible damage. Occasionally, separation of the parenchyma adjacent to fiber occurred due to the dissolution of the compound middle lamella. Ray parenchyma cells showed several boreholes having irregular shapes and sizes. Enlargement of the pits in axial and ray parenchyma was present in all the samples investigated. Xylem fibers were the most susceptible cell type and developed several tunnels through the S_2 layer. Tunnels formed in the S_2 layer of the fiber wall by the mycelia showed L- and/or T-bending. The diameter of the tunnels started narrow, increasing in size as the tunnels extended into the S_3 layer. In some instances, complete removal of the S_3 layer and fusion of the tunnels with the fiber lumen appearing as U-shaped erosion troughs was observed. At the advanced stage of decay, extensive damage was observed in the vessel walls, leaving the middle lamella and wall layer facing the vessel lumen intact. In conclusion the anatomical characteristics observed in the present study suggests that *X. polympoha* is an aggressive saprobe with strong ligninolytic activity causing soft rot type 2 decay in the wood cell wall of *Lannea coromandelica*.

Keywords: Secondary xylem, soft rot, wood damage, wood degradation

ÖZ

Xylaria polymorpha mantarının sert ağaçlarda kök çürüklüğüne neden olduğu bilinmektedir. Bu çalışmada, *X. polymorpha* ile enfekte olan Lannea coromandelica (Hint Dişbudak ağacı) türü ağaçlarında kök çürüklüğü hastalığı ile yumuşak bir çürük bozunması olduğu tespit edilmiştir. Parlak alan mikroskobu, konfokal mikroskobu ve taramalı elektron mikroskobu ile yapılan incelemelerde mantar miselyumunun fiber duvarın S_2 katmanına nüfuz ettiği, eksenel paranşimde çok fazla görünür hasar olmadığı ve nispeten dirençli olduğu görülmüştür. Bazen, liflere komşu paranşimlerin ayrılması durumu orta lamel erimesinden kaynaklanabilmektedir. Işın paranşim hücreleri, düzensiz şekil ve boyutlara sahip birkaç delik oluşturduğu görülmüştür. İncelenen tüm örneklerde eksenel ve ışın paranşiminde çukurların büyüdüğü tespit edilmiştir. Ksilem liflerinin en duyarlı hücre tipi olduğu ve S_2 katmanı boyunca birkaç tünel geliştirdiği görülmüştür. Miselyumun lif duvarının S_2 tabakasında oluşturduğu tünellerde L- ve / veya T-eğilmesi oluşmuştur. Tünellerin çapının daralmaya başladığı ve S_3 katmanına doğru genişlemesi ile boyutlarının arttığı gözlenmiştir. Bazı durumlarda, S_3 katmanının tamamen kaldırılması ile tünellerin U-şekilli erozyon çukurları olarak görünen fiber lümen ile kaynaşması gözlemlenmiştir. Çürümenin ileri safhalarında damar duvarlarında, orta lamel ve damar lümenine bakan duvar tabakasının bozulmadığı ancak büyük hasar oluştuğu gözlenmiştir. Sonuç olarak, bu çalışmada gözlemlenen anatomik özelliklerde, *X. Polympoha* mantarının, *Lannea coromandelica* ağaç türünde, ahşap hücre duvarında yumuşak çürüklüğe (tip 2) neden olan güçlü ligninolitik aktiviteye sahip olan agresif bir saprob organizması olduğunu göstermektedir.

Anahtar Kelimeler: Sekonder ksilem, yumuşak çürüklük, ahşap hasarı, odun bozunması

INTRODUCTION

Lannea coromandelica (Houtt.) Merr., commonly known as Indian ash tree, is a hardwood tree widely distributed in tropical Asia. It is popular throughout Indian literature for the medicinal value of its bark and leaves (Kaur et al., 2012). It is a hardwood species that is preferred for use in the production of bleachable pulp as well as in the manufacture of grain pounders, oil presses, plywood, block-

boards, scabbards, light furniture, packing cases, spear shafts, wheel-spokes, etc., (Gamble 1972; Nazma et al., 1981). It is also used in construction and the manufacture of agricultural implements (Basri and Hadjib, 2005; Rahman et al., 2013; Vijigiri and Sharma, 2012).

In August 2011, some *L. coromandelica* trees in the Junagadh forest were observed to be wilting with subsequent death occurring in December of the same year. At this time it was observed that the dead trees had large, club-shaped fruiting bodies which indicated the involvement of fungi in the wilting disease. Since then, trees of this species have been under observation. In 2012, the same wilting symptoms were reported in more *L. coromandelica* trees. By August 2013, there was a continued increase in the incidence of the suspected fungal disease in *L. coromandelica* and a few *Bombax ceiba* trees. The fungus was isolated from the infected wood samples and identified as *Xylaria polymorpha* using morphotaxonomic studies of the fruiting bodies.

Xylaria polymorpha causes root rot and the leaves of the infected trees to dry out permanently and fall off (Anonymous, 2008; Proffer, 1988). It is one of the few ascomycetes species that can cause the degradation of wood belonging sugar maple (*Acer saccharum*) and boxelder maple (*Acer negundo*) (Canadian Forest Service, 2012) and causes root rot in *L. coromandelica*. Root rot caused by the same fungus has also been reported

Figure 1. Fruiting bodies of *X. polymorpha* growing on the main trunk of *L. corromandelica*. Figure not to scale

in black locust (*Robinia pseudoacacia*), elm (*Ulmus* spp), honey locust (*Gleditsia triacanthos*), maple (*Acer* spp), oak (*Quercus* spp), hickory (*Carya* spp), sassafras (*Sassafras albidum*), walnut (*Juglans* spp), and beech (*Fagus* spp) (Hartman et al., 2008). Infected trees show an off-white decay and a gradual decline in vigor that eventually leads to the collapse of the weakened tree (i.e. typical features of root rot). Several club-shaped, large fruiting bodies are usually observed at ground level on the main trunk of infected trees (Hartman et al., 2008). Fungal infection is thought to take place when infected roots come into contact with healthy roots. The mechanism of mortality in trees infected with *X. polymorpha* has been extensively studied in Western tree species (Hartman et al., 2008; Proffer, 1988). However, no information is available on the pattern of wood decay caused by the fungus after the death of the trees. Therefore, in the present study, samples of the dead trees were used to study the pattern of wood decay caused by *X. polymorpha*. The isolated fungus was also inoculated onto *L. coromandelica* wood blocks for 120 days to confirm whether the pattern of degradation was similar to that observed in naturally infected trees.

Delignification is considered to be one of the important aspects of wood decay and therefore, the ligninolytic activity of fungus plays a pivotal role in their wood degradation ability. The analysis of lignin distribution patterns among different cell types in the infected wood is an effective method to assess the ligninolytic properties of fungus. Since lignin has a broad fluorescence emission range and can be excited by both UV and visible light, confocal microscopy has become an indispensable tool in the study of lignin distribution patterns in xylem cells (Donaldson et al., 2010; Donaldson and Radotic, 2013). As a commercially important wood species, assessing the extent of xylem cell wall alterations of *L. coromandelica* infected by *X. polymorpha* is necessary to understand the usefulness of the infected timber. The present study is aimed at understanding the pattern and extent of alterations in the cell wall structure, as it relates to delignification, in *L. coromandelica* infected with *X. polymorpha*.

MATERIALS AND METHODS

Source of Material
Samples of dead *L. coromandelica* (Houtt.) Merr., trees infected with *X. polymorpha* (Figure 1) were collected from a naturally growing population in Sarkhadiya Hanuman (21°32'11.13 "N, 70°33'51.75 "E) in the Girnar forest, Gujarat State (Figure 2). Four wood blocks adjacent to fungal fruiting bodies measuring 60×20×60 mm in height, width, and depth respectively were excised from the main trunk of 5 individuals by using a chisel and hammer. The wood blocks were packed in sterile polyethylene bags and transported to the laboratory. For the microscopy, samples were fixed in Formaldehyde-Acetic acid-Alcohol (FAA) (Berlyn and Miksche, 1976), aspirated with a vacuum aspirator (Millipore, Germany) to remove air from the wood while the rest of the wood blocks were used for the isolation of fungus. After 24 h of fixation, samples were transferred into 70 % alcohol for further processing and storage.
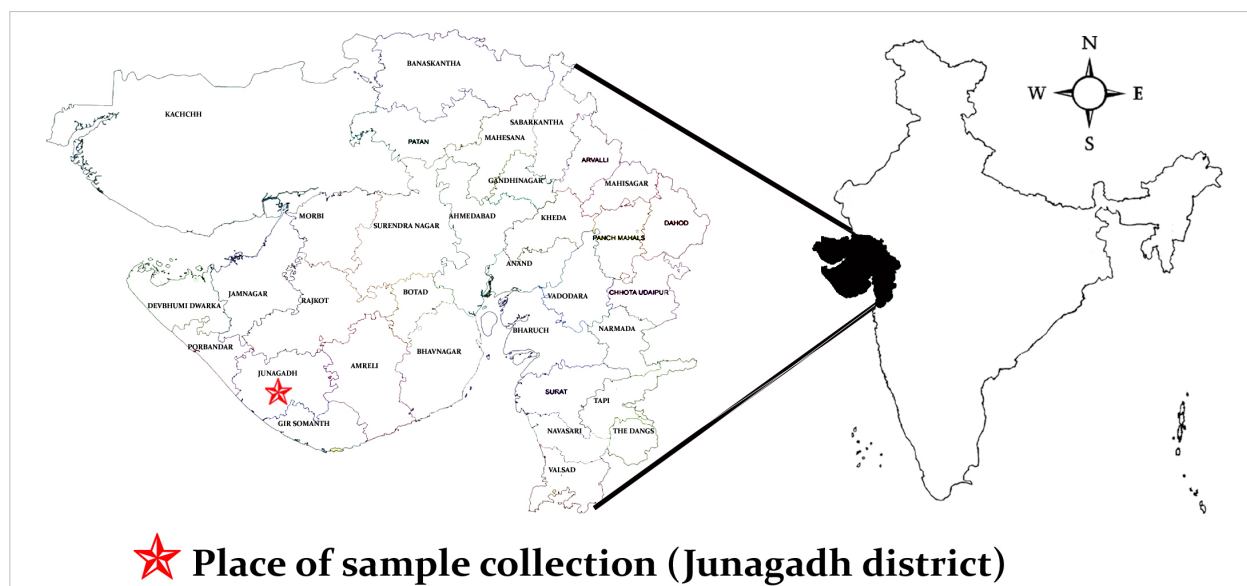
Figure 2. Distribution of *L. coromandelica* in Girnar forest of Gujarat state

Isolation and Identification of Fungus

Small pieces of unfixed wood samples were soaked in water to restore the moisture content of the wood. The moisturized wood was sterilized with 0.1% $HgCl_2$ for 40–45 seconds with intermediate washing by sterile distilled water (after every 15 seconds) followed by treatment with 70% ethanol for a few seconds. After sterilization, the wood pieces were inoculated onto 2.5% Malt Extract Agar media and incubated at room temperature. Pure cultures were established by serial transfer and cultures were maintained at 4°C.

Sectioning and Light Microscopy

The FAA fixed wood blocks were washed in distilled water and 10–15 μm thick sections were obtained in transverse, tangential, and radial view using a sliding microtome. Severely degraded wood samples were hand sectioned and stained with 0.05% aqueous toluidine blue O (Berlyn and Mikshe, 1976). The stained sections were mounted on 50% aqueous glycerol, observed and micro-photographed using a *Leica* DM 2000 microscope attached with a Canon DC 150 Digital Camera (Germany).

Maule's reaction was used (Meshitsuka and Nakano, 1979) for localizing different lignin monomers. Transverse sections were stained in 1% $KMnO_4$ for 2–3 minutes, washed in distilled water, immersed in 3–5% HCl, washed in D/W, and then treated with a few drops of ammonium hydroxide. Syringil lignin gives a reddish color while guaiacyl lignin gives a yellowish-brown color. Sections were observed and photographed immediately after the staining.

Confocal Laser Scanning Microscopy (CLSM)

Samples were washed in water followed by 0.01M phosphate buffer (pH 9.0). Hand sections (approximately 40-80 μm thick) were taken from the wood block and mounted on Fluoroshield mounting medium (Sigma, Germany). Slides were examined with a Zeiss confocal laser scanning microscope using a krypton/argon laser emitting at wavelengths of 488 and 568 nm (Donaldson and Lausber, 1998). For localization of fungal mycelia, sections were mounted on a clean glass slide with a drop each of calcofluor white and 10% potassium hydroxide (Kitin et al., 2010) followed by observation at blue excitation wavelengths (λexc=300–440 nm).

Scanning Electron Microscopy (SEM)

For SEM observations, wood samples were fixed in 2.5% glutaraldehyde in 0.2M phosphate buffer (pH 7.2) overnight. Samples were cut into small blocks of 2–3 mm thickness using a sharp razor blade, dehydrated in an acetone-isoamyl alcohol series, and coated with gold using a Quorum Sputter coater, Model SC 7610. Observations were then made with an LEO 440i SEM at 10 kV.

RESULTS

Structure of Secondary Xylem

The secondary xylem of *L. coromandelica* was diffuse-porous with an indistinct growth ring. The secondary xylem was composed of axial and ray parenchyma cells, vessels, and fibers. The axial parenchyma was vasicentric and arranged in narrow bands forming tangential lines of one to two cells wide (Figure 3a) and possessed oval to circular simple pits. Ray parenchyma cells were uni-multiseriate, heterocellular with oval to polygonal clusters of ray cells. They were 300 to 620 (±48.392) μm in height and 30 to 50 (±7.778) μm in width. Vessels were mostly solitary but radial multiples of 2–3 vessels were also observed. They were oval to oblong in outline with a simple perforation plate on the transverse end walls. Parenchyma cells formed a 1–2 cell wide sheath around them. Vessel elements were 325 to 450 (±9.538) μm in length and 120 to 207 (±19.686) μm in width. Fibers were thick-walled and septate with obliquely ori-

ented simple pits. They measured about 594 to 752 (±16.729) μm in length and 19.8 to 24.7 (±1.275) μm in width.

Light Microscopy

The transverse sections stained with toluidine blue O revealed that the tangential band of cell wall breaks across the xylem. The ray and axial parenchyma showed cell wall breaks only in these tangential bands (Figure 3a). On the other hand, the thick-walled fibers showed a large number of boreholes in the cell corners and much of the S_2 layer of the secondary wall (Figure 3b). The tangential longitudinal section showed the extension

of the boreholes across the radial wall (Figure 3c). The separation of fibers and parenchyma cells indicated the depolymerization of the compound middle lamella region (Figure 3d, e). The tangential sections showed that the separation of cell walls extended to the S_1 and S_2 layer region (Figure 3f). The space created by cell wall separation facilitated the upward and/or downward movement of fungal hyphae (Figure 3e). Hyphae entered into the parenchyma cells through the cell wall pits; while passing through, the hyphae adjusted its diameter becoming narrower (Figure 3e). The mycelia grew on the cell wall and remained
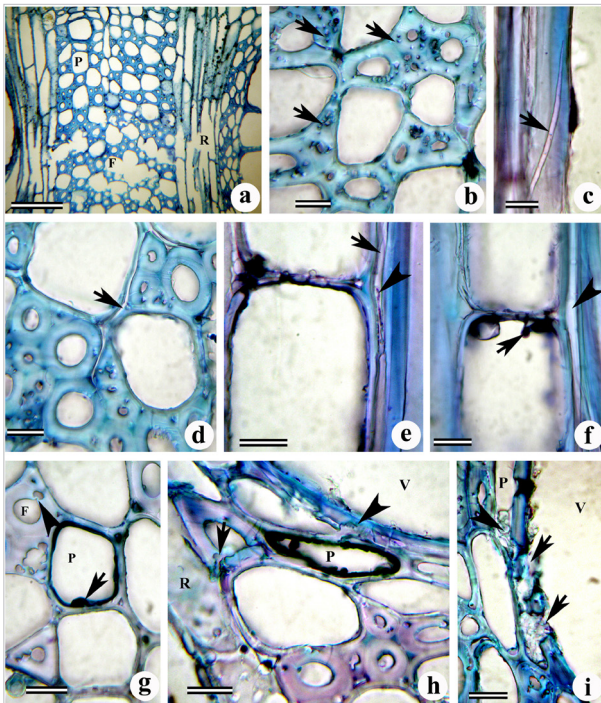

Figure 3. (a-i). Transverse (a, b, d, g-i) and radial longitudinal (c, e, f) sections from the wood of *L. coromandelica* infected by *X. polymorpha*. (a) Extensive damage to the cell wall of fiber (F) and ray (R). Note less damage to the thin-walled axial parenchyma (P). (b) A longitudinal borehole formed across the tangential wall of fiber (arrows). (c) Erosion channels formed in the secondary wall of fibers (arrow). (d) Separation of middle lamella between fiber and parenchyma cells (arrow). (e) A large gap formed (arrow) near the middle lamella region between the fiber and parenchyma cells. Arrowhead indicates the fungal mycelia passing through the degraded region of the cell wall. (f) Fungal mycelia passing through the pits between parenchyma cells (arrow). Note the narrowing of the hyphal body near the pit. Arrowhead indicates the large erosion channel formed in the fiber wall. (g) Fungal mycelia attached to the inner wall of the parenchyma cell (P). Arrowhead indicates the erosion channels formed by T-tunneling through the fiber (F) wall. (h, i) Extensive degradation and breaking of the vessel (V) wall (arrows). Arrowhead indicates the fungal mycelia in the paratracheal parenchyma cells (P).
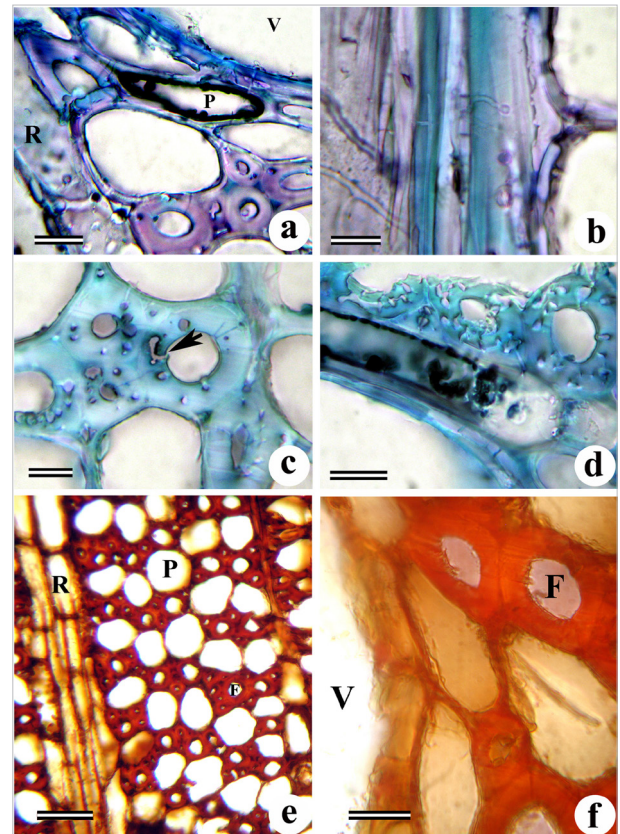*Scale bars:* a=50 μm; b-I=25 μm

Figure 4 .a-f. Transverse (a,c-f) and tangential longitudinal sections (b) of the wood of *L. corromandelica* infected by *X. polymorpha* (a-d, Toluidine blue staining). e-f (Maule's reaction). (a) A degraded wall between ray (R) and fiber. Note the fungal mycelia migrating into the adjacent paratracheal parenchyma (P) attached to the inner wall. Arrowhead indicates the erosion of the vessel (V) wall adjacent to the fungus inhabited parenchyma. (b) Fiber wall showing T-shaped tunneling (arrow). (c) L- or J-shaped tunneling in the secondary wall of fiber. (d) Fiber wall during the advanced stage of decay showing merging of numerous boreholes. (e) Fibers (F) showing more distribution of syringyl lignin units (reddish color). Note the axial parenchyma (P) and ray parenchyma (R) with brownish cell walls indicating more guaiacyl units. (f) Vessel (V) wall showing a negative color reaction (arrow) indicating more guaiacyl units. Note the reddish colored fiber (F) wall due to a higher amount of syringyl units.
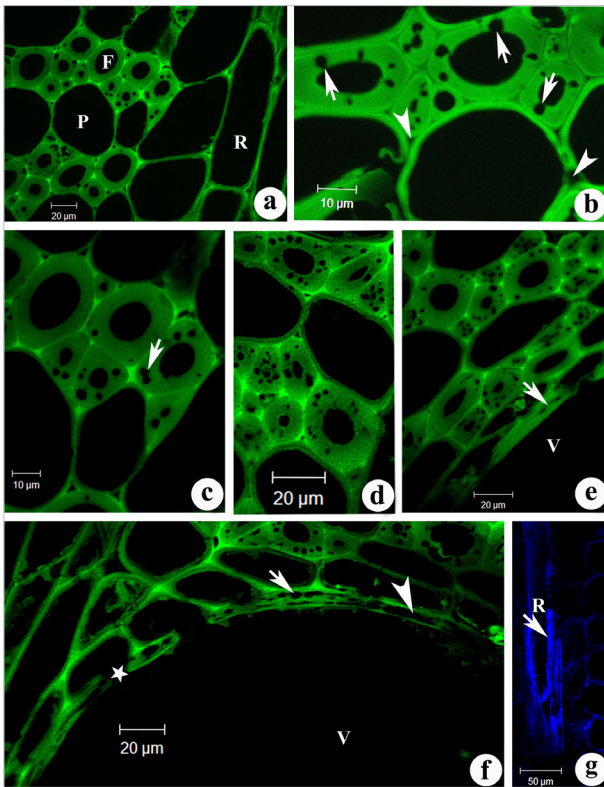*Scale bars:* a-f=25 μm

Figure 5. a-g. Confocal images of transverse sections from the wood of *L. coromandelica* infected by *X. polymorpha*. (a) High auto-fluorescence from the cell corners and compound middle lamella region of cells due to a high concentration of condensed lignin. Note the formation of erosion channels in the thick secondary wall of fiber (F) while there is relatively less damage in the thin-walled axial parenchyma (P) and ray parenchyma (R). (b) Regions of cell wall separation at delignified compound middle lamallae showing weak fluorescence. Note the secondary wall of fibers showing the beginning regions of T-tunneling (arrows). Arrowheads indicate the lack of fluorescence from the compound middle lamella of cells undergoing separation. (c) The non-fluorescent gaps formed due to large erosion channels (arrow) in the inner secondary wall of fibers through the joining of adjacent channels. (d) The sieve-like appearance of fiber secondary wall at an advanced stage of decay due to extensive tunneling. (e) High fluorescence from the vessels (V) due to the distribution of condensed lignin throughout the wall. The lack of fluorescence near the middle lamella region indicates the spreading of pit erosion (arrow). (f) Lack of fluorescence from the pockets of vessel (V) wall indicating extensive pit erosion (arrow) and subsequent secondary wall degradation during the advanced stage of decay resulting in large erosion channels (arrowhead). The asterisk indicates the broken wall between the vessel and paratracheal parenchyma cells. (g) The calcofluor white stained section showing fluorescence from fungal hyphae (arrow) in the ray cell (R).
Scale bars: a, d-f=20 μm; b, c=10 μm; f=50 μm

attached to the inner wall area (Figure 3g). Mycelia traveled radially through the vessels and colonized the vessel-associated parenchyma (Figure 3h). The pits in the vessels underwent severe degradation and expansion of the pit erosion channels into secondary wall regions leading to a complete break in the walls in several regions (Figure 3h). The migration of fungal mycelia into the various cell types of the secondary xylem was achieved by tunneling through the cell wall (Figure 4a). Boreholes and the tunneling activity of mycelia were observed only in the thick-walled elements such as fibers and vessel elements in advanced stages of decay. However, similar tunnels were absent in the axial parenchyma. Mycelia tunneled transversely through the cell walls and either underwent branching and formed a T-shaped tunnel (Fig. 4b) or bent vertically or tangentially to form L- or J-shaped tunnels (Figure 4c). Sometimes several mycelia combined or branched variously to form tunnels of many different shapes (Figure 4d).

Histochemical Analysis of Lignin

The syringyl and guaiacyl monomer ratio in wood elements was used to determine variations in fungal degradation patterns. The results of Maule's reactions revealed that the secondary wall of the fibers was rich in syringyl monomer units while vessels had a greater proportion of guaiacyl units in the cell walls (Figure 4e, f).

CLSM Analysis

The appearance of auto-fluorescence at 488 nm (blue excitation wavelength) is associated with lignin. The examination of infected xylem using blue excitation wavelengths with green light showed greater fluorescence from the middle lamella regions of fibers and parenchyma cells while the secondary wall region was characterized by relatively less fluorescence, indicating the presence of higher amounts of condensed lignin units in the middle lamella region (Figure 5a). The boreholes in the fiber secondary wall were more distinct by the nonexistence of fluorescence from these regions. The thin wall of ray and axial parenchyma showed uniform, uninterrupted fluorescence suggesting less damage to their cell wall (Figure 5a). On the other hand, the lack of autofluorescence from the cell corners and the compound middle lamella indicates lignin degradation from these regions that leads to cell separation (Figure 5b). The T-tunneling in the secondary wall of fiber was evident from the oval to circular erosion tunnels from the lumen toward the middle lamella (Figure 3b). With the progression of the decaying process, large non-fluorescent gaps were noticed in the fiber secondary wall suggesting the joining of adjacent erosion tunnels leading to a sieve-like appearance of secondary wall of fibers (Figure 5c, d). The vessel wall was characterized by high fluorescence throughout the wall compared with fiber walls and parenchyma cells pointing to the distribution of highly condensed lignin in the secondary wall (Figure 5e). The absence of auto-fluorescence as elongated patches near the middle lamella region was evidence of lignin degradation during the initial stages of wood decay and this strengthens the light microscopy observation that pit erosion spreads into the adjacent secondary wall areas (Figure 5e). In the advanced stages of vessel degradation, the

cell corners and middle lamella region remain highly fluorescent while the secondary wall region became characterized by the presence of large non-fluorescent gaps of different shapes due to extensive removal of lignin in the cell wall (Figure 5f). The
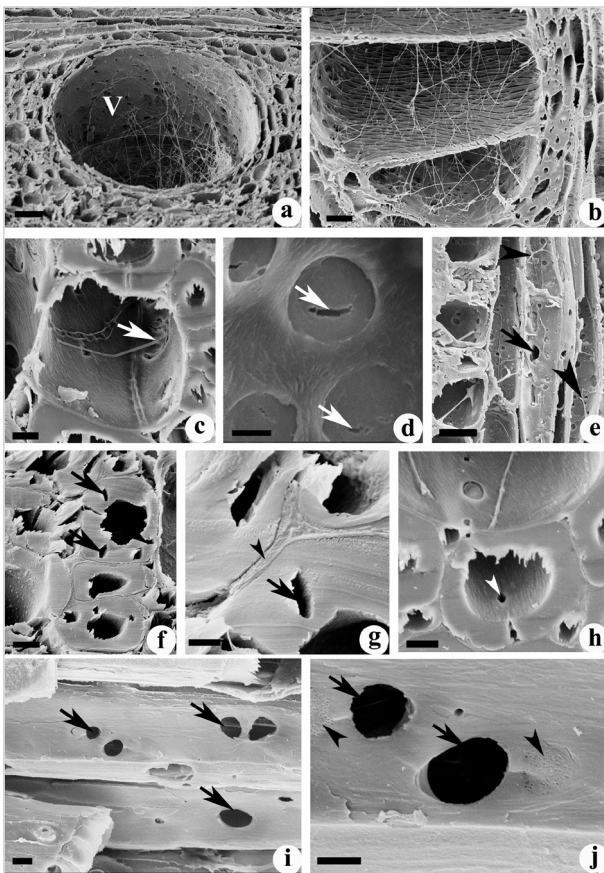

Figure 6. a-j. Scanning electron micrographs of the wood of *L. coromandelica* infected by *X. polymorpha*. (a) Vessel (V) showing colonization of the lumen by fungal mycelia. (b) Multiple vessels showing fungal hyphae passing through the inter-vessel pits. (c) Mycelia passing through the simple pits (arrow) of axial parenchyma cells. (d) Simple pits in the axial parenchyma showing erosion channels (arrows). (e) Fungal hyphae (arrowhead) proliferating through the rays. Arrow indicates the large erosion channel formed in the cell wall. (f) Fiber secondary wall showing boreholes (arrows). (g) Enlarged view of 'f' showing boreholes (arrow) located in the S2 layer of fiber. Arrowhead indicates the compound middle lamella region. (h) The L-bending mode of borehole formation in fiber. Arrowhead indicates the initiation site of a borehole from the luminal side. Note the middle layer of the secondary wall in the transverse view showing a borehole indicating the progression of wall decay in a tangential direction through the S2 layer. (i-j) Radial longitudinal section showing boreholes in fiber wall (arrows). Arrowheads indicate the regions undergoing erosion.
Scale bars: a, c, f, h=6 μm; b=40 μm; d, g, j=2 μm; e=20 μm; i=4 um

regions of initial degradation showed complete removal of wall polymers and resulted in cell wall break in these regions (Figure 5f). The intense fluorescence from the cell lumen following calcofluor white staining revealed the presence of fungal mycelia in non-contact rays (Figure 5g).

Scanning Electron Microscopy
Similar to bright-field and fluorescence microscopy, SEM analysis showed colonization of the vessel lumen by fungal mycelia (Figure 6a). In radial or tangential vessel multiples, the mycelia traversed through inter-vessel pits (Figure 6b). Similarly, in axial parenchyma, the presence of hyphae attached to the inner wall which later migrated to adjacent cells through pits without damaging the cell walls was observed (Figure 6c). However, erosion channels were seen predominantly in the simple pits (Figure 6d). The proliferation of fungal colonization in a radial direction was evident from the migration of mycelia through simple pits and by the formation of boreholes in the ray cell wall (Figure 6e). Several boreholes were noticed in the secondary wall of fibers which were located in the S$_2$ layer region of the walls (Figure 6f, g). As mentioned earlier, after tunneling through the cell wall, mycelia bent to form L-shaped tunnels. The bending pattern of tunnels was evident from the formation of boreholes in transverse directions from the luminal side and the appearance of holes in the S$_2$ layer in the region above the initiation site (Figure 6h). The radial longitudinal view also showed the presence of large erosion channels in the fiber walls (Figure 6i). The thinning of the cell wall by complete erosion of S3 layer and part of S2 layer and the formation of minute holes were apparent in the regions were erosion was progressing in the fibers (Figure 6j).

DISCUSSION
Xylaria is the largest genus of the family Xylariaceae, comprising about 300 species of stromatic pyrenomycetes (Fournier et al., 2011). They are important components of the terrestrial ecosystem where they survive as saprophytes and play a vital role in the decomposition of plant debris. Some members degrade wood, as well as being plant pathogens that cause root rot disease in forest and orchard trees (Fournier et al., 2011; Hartman et al., 2008; Okane et al., 2008; Proffer, 1988). Reports indicate that the majority of the members of the family, including *Xylaria*, occur ubiquitously as endophytes of vascular plants and lower plants such as liverworts and algae (Arnold et al., 2000; Davis et al., 2003; Sturz et al., 2000; Tenguria et al., 2011). *Xylaria polymorpha* is a well-known pathogen that causes root rot disease in several tree species growing in the USA, Europe, and Canada (Proffer, 1988; Hartman et al., 2008). It infects trees through the root system and infected plants show typical symptoms of root rot that consequently lead to the death of the tree (Hartman et al., 2008). Similar symptoms were observed in the present study. *Xylaria polymorpha* shown to have strong ligninolytic and hydrolytic activity (Liers et al., 2006, 2007; Pointing et al., 2005), as well as some novel glycoside hydrolases that facilitate the effective degradation of lignocelluloses (Nghi et al., 2012). The mechanism of infection and disease symptoms of the infected trees were described by Hartman et al., (2008). However, information on the characteristics of wood damage after tree mor-

tality is lacking. Therefore, the present study attempts to show the structural alterations in the cell wall as a result of fungal infection.

Available information has shown that members of ascomycetes produce a soft pattern of wood decay (Worall et al., 1997). In hardwoods, all the constituents of the cell wall may be degraded in soft rot but the carbohydrates are more susceptible (Worall et al., 1997). Depending on which component of the cell wall is damaged, these fungal infections have been classified as white rot, brown rot, and soft rot. Soft rots usually occur in dry environments and the decayed wood may macroscopically appear similar to brown rot (Blanchette, 2000). *In vitro* experiments on the wood decay pattern in three hardwood species infected by *X. hypoxylon,* revealed a combination of both soft and white rot characteristics (Koyani et al., 2017). *Lannea coromandelica* wood infected by *X. polymorpha* forms boreholes and erosion tunnels in the S$_2$ layer of the fiber wall, which is characteristic of soft rot pattern. Similar characteristics of soft rot were also reported by earlier studies (Blanchette, 2000; Fazio et al., 2010; Nilsson et al., 1989; Schwarze, 2007). Formation of longitudinal tunnels in the wood of *L. coromandelica* infected with *X. polymorpha* suggests that thick-walled elements such as fibers and vessels are more susceptible to attack, while thin-walled cells like axial and ray parenchyma show less cell wall damage. The relatively lower amount of cell wall polymers in ray and axial parenchyma and the presence of phenolic polymers in the living parenchyma may result in their lower vulnerability during the decaying process. However, when the extension of decay is tangential or radial, these cells may also undergo degradation. The diffuse type of axial parenchyma cells and contact rays have shown degradation and breakage of the cell wall that facilitated the migration of mycelia into adjacent fibers and vessels. The thick secondary wall is known to be rich in wall polysaccharides mainly cellulose, hemicellulose, and phenolic polymer lignin. Our light microscopy analysis revealed a large number of boreholes in the middle layer of the fiber secondary wall. Two types of soft rot has been identified based on the anatomical charecteristics of wood decay following fungal invasion. The type 1 decay is due to the repetitive start and stop pattern of hyphal growth results in gradual breakdown of the secondary wall layer of wood cells while discrete notches of cell wall erosion by hyphal movement within the lumen along with cavities formed within the cell wall leading to the formation of erosion troughs is termed as type 2 soft rot decay (Schwarze, 2007). The T-branching and L-bending patterns are characteristic of soft rot (type 1) while the formation of diffuse cavities similar to white rot is characteristic of type 2 soft rot. In the present study, fiber walls showed the formation of T-branching and L-bending patterns. The fiber secondary wall, especially the thick S$_2$ layer is known to be more prone to degradation because of a higher amount of hydrolyzable cellulosic polysaccharides and lower lignin content while the lignin-rich compound middle lamellae and S$_3$ wall layer are resistant to decay. The present study showed degradation of the compound middle lamella which resulted in the separation of cells suggesting that the lignin-rich regions of the cell wall can also be degraded by *X. polymorpha*.

Compared to other xylem cell types, the vessels are characterized by a relatively higher distribution of condensed lignin throughout the cell wall (Saka, 2000). From a functional perspective, the highly condensed lignin in vessel walls has been attributed to increased strength that is useful in withstanding the compression forces caused by transpiration stress (Pramod et al., 2013; Xu et al., 2006). Additionally, the increased strength may be important against stem torsion and bending as well as providing resistance to biodegradation by fungi. The CLSM analysis of the infected *L. coromandelica* wood showed a high intensity of auto-fluorescence throughout the vessel wall and compound middle lamella of other cell types. Maule's reaction confirmed the presence of more syringyl units in the fiber secondary wall and more guaiacyl units in the cell wall. The guaiacyl residues absorb more light than syringyl residues and are therefore more fluorescent (Micco and Aronne, 2007). The early stages of lignification in Aspen (*Populus* spp) fibers are marked by the distinct incorporation of guaiacyl subunits in the middle lamella region while the incorporation of syringyl units is increased in the secondary layers during later stages (Grünwald et al., 2002). Therefore, the observed high auto-fluorescence from the vessel wall and compound middle lamella may be due to the presence of a high concentration of condensed, guaiacyl lignin units, and this lignin distribution pattern is responsible for the decay resistance in these wall regions. A similar lignin distribution has been reported in literature and it has been concluded that the persistence of vessels may be due to a higher content of guaiacyl monomer content (Blanchette et al., 1987, 1988; Iiyama and Pant, 1988; Koyani et al., 2010; Nakano and Meshitsuka, 1978; Sanghavi et al., 2013; Schwarze et al., 2000). Confocal microscopy showed the absence of auto-fluorescence from the compound middle lamella of cells undergoing separation indicating the removal of lignin. The disappearance pattern of auto-fluorescence during sequential stages of vessel wall decay suggests that the lignin degradation begins in the compound middle lamella region through pit erosion and spreads into adjacent secondary wall layers.

CONCLUSION

Fruiting bodies and fungi isolated from infected samples confirmed the infectious species as *X. polymorpha*. The *in vitro* wood decay experiment using isolated organism from the infected wood induced characteristic features of soft rot, including the formation of boreholes of irregular size and shape in the S$_2$ layer of the cell wall. Compared to thin walled parenchyma cells, xylem fibers with thick secondary wall were the most susceptible cell types and developed several tunnels through the S$_2$ layer. Tunnels formed in the S$_2$ layer of the fiber wall by the mycelia showed L- or T-bending. Initially, the tunnels were narrow in diameter but increased in size as they extended into the S$_3$ layer. Occasionally complete removal of the S$_3$ layer and fusion of the tunnels with the fiber lumen appeared as U-shaped erosion troughs. At advanced stages of decay, extensive damage was observed in the vessel walls, leaving the middle lamella and wall layer facing vessel lumen intact. The degradation of the cell wall and middle lamella of xylem cells suggest that *X. polymorpha* is an aggressive saprobe with strong ligninolytic activity.

REFERENCES

- Anonymous, 2008. Medicinal Mushrooms: Investigating bioactive compounds from kingdom fungi. Available from: http://healing-mushrooms.net/archives/xylaria-polymorpha.html
- Arnold, E., Maynard, Z., Gilbert., G.S., Coley, P.D., Kursar, T.A., 2000. Are tropical fungal endophytes hyperdiverse? *Ecology Letters* 3(4): 267-74. [Crossref]
- Basri E., Hadjib, S., 2005. Basic properties in relation to drying properties of three wood species from Indonesia. *Journal of Forestry Research* 2(1): 49-56. [Crossref]
- Berlyn, G.P., Miksche, J.P., 1976. Botanical microtechnique and cytochemistry. The Iowa State University Press, Ames, Iowa, pp. 326. [Crossref]
- Blanchette, R.A., Obst, J.R., Hedges, J.I., Weliky, K., 1988. Resistance of hardwood vessels to degradation by white rot Basidiomycetes. *Canadian Journal of Botany* 66: 1841-1847. [Crossref]
- Blanchette, R.A., Otjen, L., Carlson, M.C., 1987. Lignin distribution in cell walls of birch wood decayed by white rot basidiomycetes. *Phytopathology* 77(5): 684-690. [Crossref]
- Blanchette, R.A., 2000. A review of microbial deterioration found in archaeological wood from different environments. *International Biodeterioraton and Biodegradation* 46: 189-204. [Crossref]
- Canadian Forest Service, 2012. *Xylaria* root rot - Trees, insects and diseases of Canada's forests. Available from: http://www.tidcf.nrcan.gc.ca/diseases/factsheet/32
- Davis, E.C., Franklin, J.B., Shaw, A.J., Vilgalys, R., 2003. Endophytic *Xylaria* (Xylariaceae) among liverworts and angiosperms: phylogenetics, distribution, and symbiosis. *American Journal of Botany* 90(11): 1661-1667. [Crossref]
- Donaldson, L.A., Radotic, K., 2013. Fluorescence lifetime imaging of lignin autofluorescence in normal and compression wood. *Journal of Microscopy* 251(2): 178-187 [Crossref]
- Donaldson, L.A., Lausberg, M.J.F., 1998. Comparison of conventional transmitted light and confocal microscopy for measuring wood cell dimensions by image analysis. *International Association of Wood Anatomists Journal* 19(3): 321-336. [Crossref]
- Donaldson, L.A., Radotic, K., Kalauzi, A., Djikanovic, D., Jeremic, M., 2010. Quantification of compression wood severity in tracheids of *Pinus radiata* D. Don using confocal fluorescence imaging and spectral deconvolution. *Journal of Structural Biology* 169(1): 106-115. [Crossref]
- Fazio, A.T., Papinutti, L., Gómez, B.A., Parera, S.D., Rodríguez, R.A., Siracusano, G., Maier, M.S., 2010. Fungal deterioration of a Jesuit South American polychrome wood sculpture. *International Biodeterioration and Biodegradation* 64: 694-701. [Crossref]
- Fournier, J., Flessa, F., Peršoh, D., Stadler, M., 2011. Three new Xylaria species from southwestern Europe. *Mycological Progress* 10: 33-52. [Crossref]
- Gamble, J.S., 1972. A manual of Indian timbers: an account of the growth, distribution, and uses of the trees and shrubs of India and Ceylon, with descriptions of their wood-structure. 2d ed. Dehra Dun: Bishen Singh Mahendra Pal Singh.
- Grünwald, C., Ruel, K., Kim, Y.S., Schmitt, U., 2002. On the cytochemistry of cell wall formation in poplar trees. *Plant Biology* 4(1): 13-21. [Crossref]
- Hartman, J., Beale, J., Bachi, P., 2008. Root and Collar Rots of Tree Fruits. UK Cooperative Extension Service, Plant Pathology Fact sheet. College of Agriculture, University Kentucky (PPFS-FR-T-10).
- Iiyama, K., Pant, R., 1988. The mechanism of the Maule colour reaction. Introduction of methylated syringyl nuclei in softwood lignin. *Wood Science and Technology* 22: 167-175. [Crossref]
- Kaur, R., Jaiswal, M.L., Jain, V., 2012. Preliminary pharmacognostical and phytochemical investigation of bark and leaves of *Lannea coromandelica* (Houtt.) Merrill. International *Journal of Pharmacognosy and Phytochemical Research* 4(3): 82-88.
- Kitin, P., Voelker, S.L., Meinzer, F.C., Beeckman, H., Strauss, S.H., Lachenbruch, B., 2010. Tyloses and phenolic deposits in xylem vessels impede water transport in low-lignin transgenic Poplars: A study by cryo-fluorescence microscopy. *Plant Physiology* 154(2): 887-898. [Crossref]
- Koyani, R.D., Sanghvi, G.V., Bhatt, I.M., Rajput, K.S., 2010. Pattern of delignification in *Ailanthus excelsa* Roxb, wood by *Inonotus hispidus*. *Mycology* 1: 204-211. [Crossref]
- Koyani, R.D., Pramod, S., Patel, H.R., Vasava, A.M., Rao, K.S., Rajput, K.S., 2017. Anatomical characterisaton and in-vitro laboratory decay test of different woods decayed by *Xylaria hypoxylon*. In: Pandey, KK., Ramakantha V., Chauhan, SS., Arun Kumar AN., (eds.) Wood is good: Current trends and future prospects in wood utlisation, pp 93-103. Springer Nature Singapore Pte Ltd. [Crossref]
- Liers, C., Ullrich, R., Steffen, K.T., Hatakka, A., Hofrichter, M., 2006. Minerilization of ^{14}C-labelled synthetic lignin and extracellular enzyme activities of the wood-colonizing ascomycetes *Xylaria hypoxylan* and *Xylaria polymorpha*. *Applied Microbiology Biotechnology* 69(5): 573-579. [Crossref]
- Liers, C., Ulrich, R., Pecyna, M., Schlosser, D., Hofrichter, M., 2007. Production, purification and partial enzymatic and molecular characterization of laccase from the wood rotting ascomycete *Xylaria polymorpha*. *Enzyme and Microbial Technology* 41: 785-793. [Crossref]
- Meshitsuka, G., Nakano, J., 1979. Studies on the mechanism of lignin color reaction (XIII): Maüle color reaction (9). *Mokuzai Gakkaishi* 25: 588-594.
- Micco, V.D., Aronne, G., 2007. Anatomical features, monomer lignin composition and accumulation of phenolics in 1 year old branches of the Mediterranean *Cistus ladanifer* L. *Botanical Journal of the Linnean Society* 155(3): 361-371. [Crossref]
- Nakano, J., Meshitsuka, G., 1978. Studies on the mechanism of lignin colour reaction. XII. Maule color reaction. *Mokuzai Gakkaishi* 24: 563-568.
- Nazma P., Ganapathy, P.M., Sasidharan, N., Bhat, K.M., Gnanaharan, R., 1981. A handbook of Kerala timbers. *KFRI Research Report* 9: 260.
- Nghi, DH., Bittner B., Kellner H., 2012. The Wood rot ascomycete *Xylaria polymorpha* produces a novel GH78 glycoside hydrolase that exhibits L-Rhamnosidase and feruloyl esterase activities and releases hydroxycinnamic acids from lignocelluloses. *Applied and Environmental Microbiology* 78(14): 4893-4901. [Crossref]

- Nilsson, T., Daniel, G., Kirk, T.K., Obst, J.R., 1989. Chemistry and microscopy of wood decay by some higher ascomycetes. *Holzforschung* 43(1): 11-18. [Crossref]
- Okane, I., Srikitikulchai, P., Thomas Læssøe, K.T., Sivichai, S., Hywel-Jones, N., Nakagiri, A., Suzuki, W.P.K., 2008. Study of endophytic Xylariaceae in Thailand: diversity and taxonomy inferred from rDNA sequence analyses with saprobes forming fruit bodies in the field. *Mycoscience* 49(6): 359-372. [Crossref]
- Pointing, S.B., Pelling, A.L., Smith, G.J.D., Hyde, K.D., Reddy, C.A., 2005. Screening of basidiomycetes and xylariaceous fungi for lignin peroxidase and laccase gene specific sequences. *Mycological Research* 109(1): 115-124. [Crossref]
- Pramod, S., Rao, K.S., Sundberg, A., 2013. Structural, histochemical and chemical characterization of normal, tension and opposite wood of Subabul (*Leucaena leucocephala* (Lam.) De Wit.). *Wood Science and Technology* 47(4): 777-796. [Crossref]
- Proffer, T.J., 1988. *Xylaria* root rot of urban trees caused by *Xylaria polymorpha*., *Plant Disease* 72: 79. [Crossref]
- Rahman, K.S., Shaikh, A.A., Rahman, M.M., Alam, D.M.N., Alam, M.R., 2013. The potential for using stem and branch of Bhadi (*Lannea Coromandelica*) as a lignocellulosic raw material for particleboard. *International Research Journal of Biological Sciences* 2(4): 8-12.
- Saka, S., 2000. Chemical composition and distribution. In: David N-SH. and Shiraishi, N. (eds.), Wood and cellulose chemistry, 2nd edn., Marcel Dekker, Inc. New York, pp. 51-81.
- Sanghvi, G.V., Koyani, R.D., Rajput, K.S., 2013. Anatomical characterization of teak wood (*Tectona randis* L.f.) decayed by fungus *Chrysosporium asperatum*. *Journal of Tropical Forest Science* 25(4): 547-553.
- Schwarze, F.M.W.R., Baum, S., Fink, S., 2000. Resistance of fibre regions in wood of *Acer pseudoplatanus* degraded by *Armillaria mellea*. *Mycological Research* 104(9): 126-132. [Crossref]
- Schwarze, F.M.W.R., 2007. Wood decay under the microscope. *Fungal Biological Review* 21: 133-170. [Crossref]
- Sturz, A.V., Christie, B.R., Nowak, J., 2000. Bacterial endophytes: potential role in developing sustainable systems of crop production. *Critical Reviewes in Plant Sciences* 19(1): 1-30. [Crossref]
- Tenguria, R.K., Khan, F.N., Quereshi, S., 2011 Endophytes-mines of pharmacological therapeutics. *World Journal of Science and Technology* 1(5): 127-149.
- Vijigiri, D., Sharma, P.P., 2012. Timber yielding plants and their utilities in Nizamabad district of Andhra Pradesh. *Journal of Phytology* 4(4): 17-20.
- Worall, J.J., Anagnost, S.E., Zabel, R.A., 1997. Comparison of wood decay among diverse lignicolus fungi. *Mycologia* 89: 199-219. [Crossref]
- Xu, F., Sun, R.C., Lu, Q., Jones, G.L., 2006. Comparitive study of anatomy and lignin distribution in normal and tension wood of *Salix gordejecii. Wood Science and Technology* 40: 358-370. [Crossref]